IMPERIAL COLLEGE LONDON

DEPARTMENT OF MATERIALS

MATE50003 ENGINEERING PRACTICE

Interim Report

30 May 2024

Group: G16

Project Manager: Dr Mark R Wenman

Francesca Manyonyi

Isabella Wu

Mervyn Ochoa-Dugoy

Nick Martin

Saiful Islam

Tianrui Zheng

Table of Contents

Executive Summary

This report details Group G16's process for characterising the UTEN 4 in 1 Multi-Functional High-Speed Food Processor, with the aim of defining the materials properties and manufacture history of the blender's primary components – the blades, base plate, front plate, male and female blender gears, casing, and O-ring (previously referred to as the 'rubber lining' – in order to find the root causes of the blender's failures according to user complaints in Amazon reviews as outlined in the Preliminary Report. Group 16's characterisation process is split into two sub-groups – one handling polymers and the other handling steel parts – and involves visible light microscopy (VLM), scanning electron microscopy (SEM) energy-dispersive x-ray spectroscopy (EDX), Fourier Transform Infrared Spectroscopy (FTIR), Differential Scanning Calorimetry (DSC), Vickers and Shore hardnesses, magnetism tests, and densimetry. From characterisation data, the blades were found to be 304 austenitic stainless steel; the base plate was 201 austenitic stainless steel and polyamide. The exterior was made of 430 ferritic stainless steel and acrylonitrile butadiene styrene. The male and female gears were made of nitrile butadiene rubber and polyamide respectively, while the O-ring was found to be PDMS (Polydimethylsiloxane). The whole process cost £4125, which is below the maximum £5000 budget with £875 left over but is in excess of the initial spending plan by £875. After characterisation, testing, and analysis of results, Group G16 offers improvements to the blender's design: a redesigned base plate with the O-ring eliminated entirely, redesigned blades, and a fully-polymer exterior. These improvements will have a positive impact on user safety and experience, while maintaining the low price point of the blender.

1 Introduction

The low-cost UTEN 4 in 1 blender serves as an affordable, easy-to-use product for consumers to blend food ingredients. However, as seen in Amazon reviews, users had several complaints regarding the product's components and their functionalities, which led to a poor user experience (and low ratings). Users complained of blades blending food ineffectively and snapping, the front plate overheating and denting, the base plate denting and allowing leakage into the blender's electricals, the O-ring shredding and permitting leakages, and the gears wearing out, all leading to an average lifespan of less than a year[1] – it was observed that the manufacturer aimed to sell the blender at a low price but in large volumes. To understand the cause of the blender's problems, characterization and testing of components - confirming their material makeup – was necessary to provide a thorough grasp of the structure and properties of the blender's principal components, which ultimately contribute to its overall performance[1]. Throughout the characterization window, Group G16 tested the key components mentioned in the Preliminary Report[2] and ran a logical series of experiments on two main material classes: steels and polymers[2]. Experiments involved visible light microscopy (VLM), scanning electron microscopy (SEM) energy-dispersive x-ray spectroscopy (EDX), fourier transform infrared spectroscopy (FTIR), differential scanning calorimetry (DSC), Vickers and Shore hardnesses, magnetism tests, and densimetry. It was expected for there to be faults within microstructure (phases) and composition across steel components, and likewise for bonded elements and interactions for polymers[4,5]. G16 evaluated data garnered from the experiments. The results were compared to existing materials and their industrial standards. By the end, G16 drew conclusions, criticizing and appraising the manufactured components and providing reasonable recommendations for improvements which would allow the augmented product to still remain within the UTEN blender's low price range – selling in volumes – while being worthwhile for consumers.

2 Characterisation – Experimental Details

2.1 Steels

The steel group was comprised of Nick, Francesca and Saiful, characterised three steel components of the blender: the blending blades, the base plate, and the front plate. All the samples were tested for magnetism by observing their response to a magnet.

The samples were cut into smaller pieces using a AbrasiMet 250 manual abrasive cutter then hot-mounted in cured resin moulds using the Struers Citopress 30. There were three samples made of (each) the blade and the base plate; there were two samples made of the front plate (See *Appendix 1*). Each sample was ground thrice using a MetaServ polisher (320, 600 and 1000 grit) and then polished using 3 micron and 1 micron diamond lubricants in preparation for characterisation. Finally, the samples were rinsed with distilled water and ethanol before being etched using glyceregia[3]; one sample from each steel part (i.e., one blade sample, one base plate sample and one front plate sample) was over etched (for 2min15s). The rest of the samples were etched for 1min30s.

Visible light microscopy (VLM) on an Olympus BX51 transmission/reflection microscope was used to inspect the morphology of the samples. Both sides of each sample were viewed unpolarised from 10x to 100x magnification. ImageJ[4] was used to process the images. A JEOL JS-6010PLUS/LA, 20 kV, 15mm working distance, 45nm spot size, was used to perform high-resolution scanning electron microscopy (SEM) on both sides of one blade sample and one base plate sample. Energy-dispersive x-ray (EDX) data on the elemental composition of the samples was also collected; both point EDX at three points and EDX mapping were conducted. SEM, supplemented by EDX, gave information about chemical composition. EDX data was plotted on Microsoft Excel. Vickers hardness tests were performed on the blade and the base plate using an ISO 6507/ASTM E 92. Five measurements were taken at varying points – the centre and the edges – of one sample of each part.

2.2 Polymers

The polymer group was comprised of Mervyn, Isabella and Tianrui. Two samples of each of the following components were prepared: casing, gears (male and female), O-ring and base plate. These were cut and smoothened down into approximately 1cm x 1cm (length x width) square sections using a coping saw then P80 grit sandpaper, clearing off any residue. One of each sample was taken to a germanium-tipped Agilent Cary 630 ATR-FTIR spectrometer to examine and identify the used polymers and associated bond interactions. Using its attached software, the produced IR spectrums were compared to similar known spectra as a guide. The same samples then underwent densimetry using the Ohaus Pioneer™ analytical balance, integrated with its density determination kit (Item number 80253384). Prior to testing, 150ml of distilled water was added into the provided volumetric cylinder and its temperature (in ^{o}C) and density, ρ_L was recorded. Each sample was first weighed 'in air' using the upper platform then weighed again at the platform immersed in distilled water. The attained values were put into the following density equation – based on Archimedes' principle:

$$\rho_0 = \frac{A}{A-B}(\rho_0 - \rho_L) + \rho_L$$

For the other set of prepared polymer samples, Mitutoyo HH-331 and HH-334 durometers were used to measure their Shore A and D hardness respectively, set up on a flat smooth table. After identifying, comparing and making justified analysis from FTIR, densimetry and hardness testing, the male blender gear and casing materials underwent DSC using the Mettler Toledo DSC 3 machine. Samples were prepared in crucibles with the Mettler Toledo sealing press. The polymer samples were weighed individually, aiming between 8 - 12 mg, as well as the crucible base and top

themselves summed up. Under inert liquid nitrogen settings, the male blender gear sample underwent 2 tests under 5°C per minute: -80°C - 0°C and 150°C - 200°C. Furthermore, 10°C per minute tests were conducted between 80°C and 240°C for both components. The collective data for FTIR and DSC was analysed in Origin[5], using relative peak analysis features compared to Granta EduPack Level 3 material data[6], literature values and graphs.

3 Characterisation – Results and Analysis

3.1 Steels

3.1.1 Blades

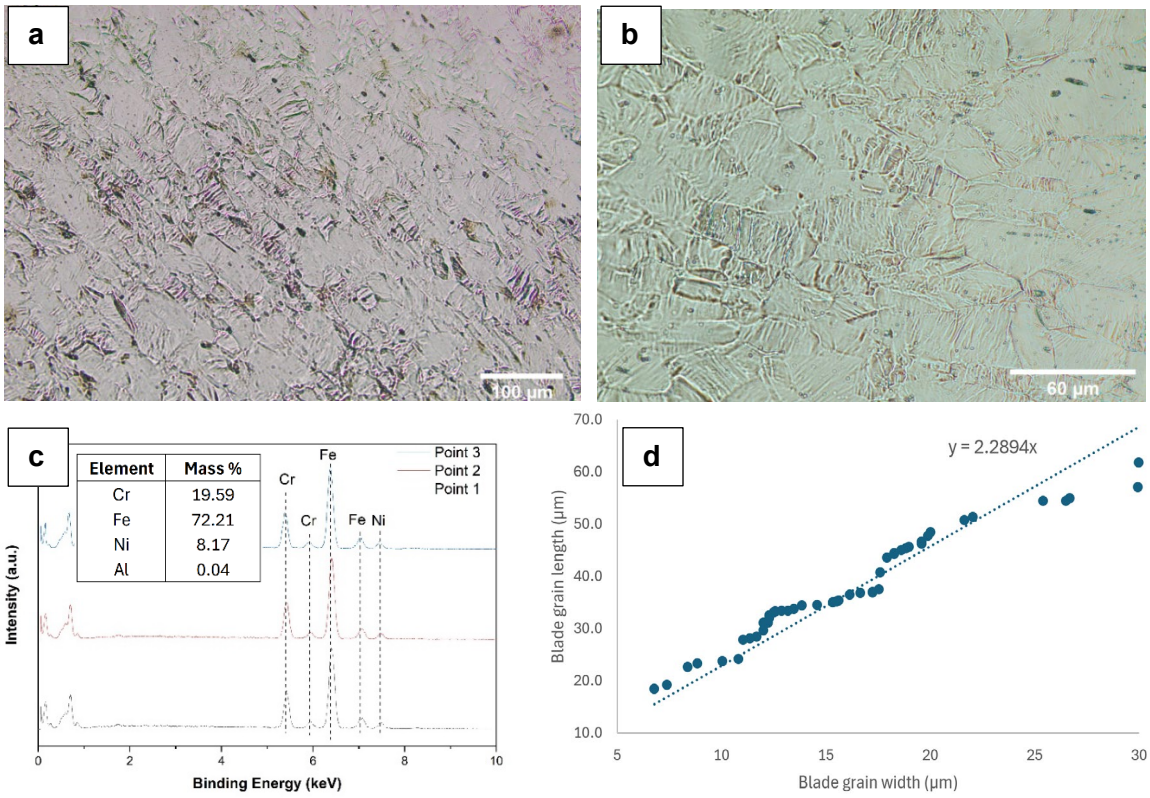

Figure 1. *(a) VLM Image of the over etched sample of the blade at 20 x magnification, with a polariser and the aperture diaphragm applied, (b) VLM Image of the over etched sample of the blade at 50 x magnification, with a polariser and the aperture diaphragm applied, (c) EDX spectrum for the blade and accompanying table of average EDX elemental mass percentages, with Boron excluded to eliminate systematic error, (d) graph of grain length against grain width as measured manually on ImageJ, showing a best fit ratio of 2.29 between the two, signifying elongated grains.*

The blade was slightly magnetic (like the base plate) suggesting an austenitic, face-centred cubic (FCC) phase[7]. Point EDX was performed on the blade to determine the elemental composition of the sample as seen in *Figure 1c* confirming that the blades are made of 304 stainless steels[8]. Nickel is introduced as a stabiliser as it helps maintain the austenitic FCC phase at lower temperatures and extends its operational temperature range[9]. An austenitic phase is ideal because it enhances toughness and ductility, allowing the steel to withstand high-speed impacts and stresses, which are typical for blender blades. Additionally, the presence of Nickel enhances the blades' corrosion resistance and makes them non-reactive, which is essential for food contact applications. Due to 304 steel's ductility and its weldability, it is easy to form into complicated shapes as seen in some of the blades[10]. 304 steel additionally forms a passive layer of chromium oxide on the surface which

prevents scratches and corrosion whilst being non-porous[11], making the blades easy to clean and thus maintaining hygiene[12].

From VLM the microstructures in *Figure 1a* and *1b* were analysed; the grain shapes from the sample suggest it was cold rolled 304 stainless steels[13]. The elongation of the grains is due to the deformation process. Cold rolling tends to refine the grain structure, leading to smaller grain sizes compared to the original material. The grain size average length was 38.2 ± 16.8 µm and width of 10.7 ± 6.7 µm. The ratio of length to width for grains as seen in *Figure 1d* is 2.29, denoting a 129% increase in length. This is on the higher end of typical values, which means the material may be at risk of defects such as buckling, wrinkling or tearing, which could have led to the damage reported by reviews[14]. The relative inhomogeneity of grain size suggests that deformation during the process was uneven resulting in different levels of strain throughout the material. The lines observed on the microstructure in *Figure 1b* running perpendicular to the boundaries across most of the grains are likely slip lines or deformation bands resulting from the cold rolling process indicating the direction of deformation[15]. The darker spots on the image may indicate areas of localised deformation, oxidation, or variations in the etching process. Additionally, the blade had an average Vickers hardness of 329 ± 17 HV, which is within expectation for cold rolled 304 stainless steels[16]. The steel would most likely undergo several manufacturing steps; first cold rolling to achieve the desired blade thickness, then cutting and bending into shape before polishing and grinding, followed by edge sharpening.

3.1.2 Front Plate

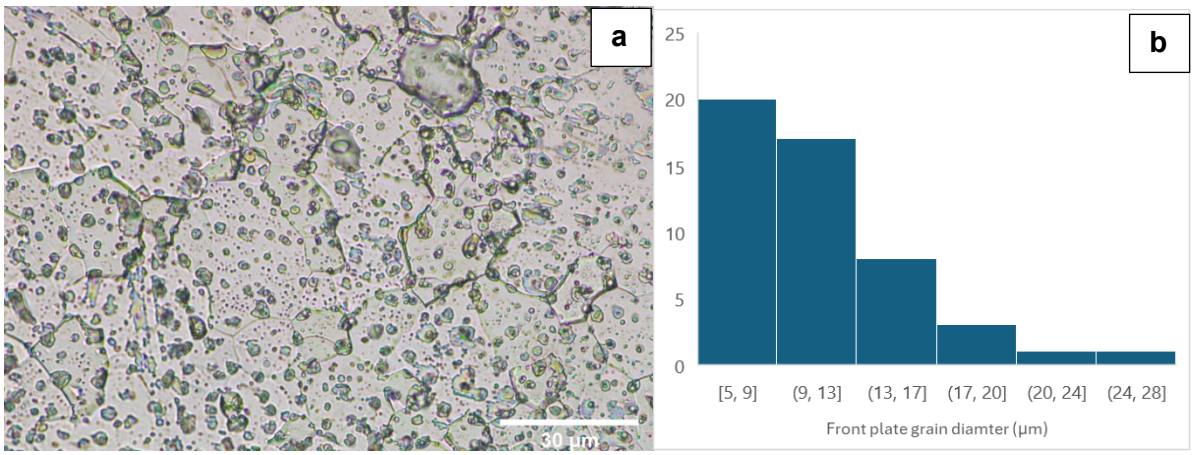

Figure 2. *(a) VLM image of the over etched sample of the front plate at 100 x magnification, with the aperture diaphragm applied, (b) histogram of the distribution of grain diameters in the front plate; 50 manual measurements taken on ImageJ.*

The front plate was magnetic, suggesting its BCC ferritic structure[17]. VLM shows that it is likely AISI 430 ferritic stainless steel due to the presence of equiaxed grains with some randomly dispersed precipitates, Chromium Carbide[18], which appear to be larger at grain boundaries as shown in *Figure 2a.* An average grain diameter of 11.2 ± 4.1 µm was calculated when 50 grains in *Figure 2a* were analysed on ImageJ (See *Figure 2b)*, as well as an average carbide diameter of 722 ± 45 nm; the average grain size falls well within the common literature value range of 7.9 to 13.4 µm[19,20]. The base plate has an average Vickers hardness of 148.7 ± 5.7 HV, which is consistent with literature values for 430 stainless steels[21]. SEM/EDX were not deemed necessary for the front plate due to it not being a key component and the group felt no further classification was of necessity.

The corrosion resistance of 430 stainless steels is typically lower than other stainless steels, especially austenitic steels in the 300 series. 430 steels are cheaper than other commonly used stainless steels (e.g., 304 steel)[22], and thus a cost-effective option to use in a cheap blender. The

thermal conductivity of 430 steels is greater than austenitic stainless steels, aiding in outward dissipation of heat from the motor to the blender's exterior. Meanwhile, the low hardness values obtained explain the frequent denting of the blender's exterior. The chromium carbides slightly increase the hardness of the steel, but also make it more brittle and susceptible to denting.

3.1.3 Base Plate (Steel Surface)

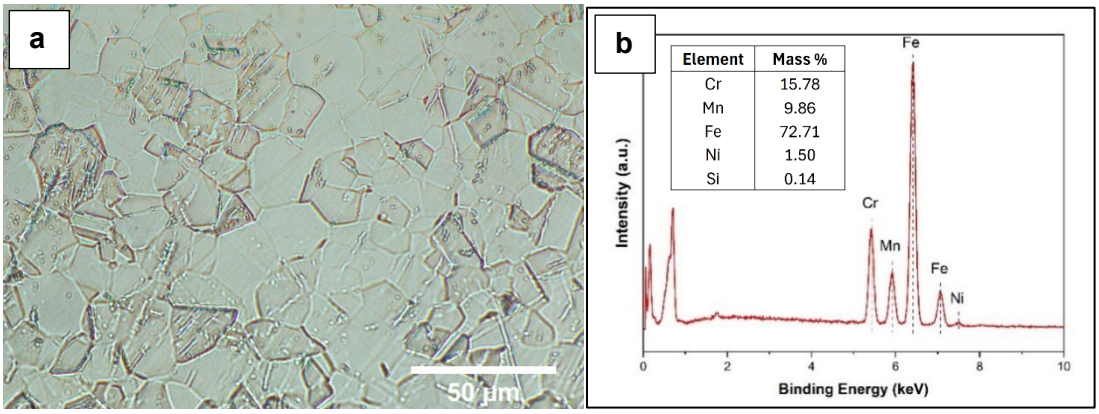

Figure 3. *(a) VLM Image of the over etched sample of the base plate at 50 x magnification, with a polariser and the aperture diaphragm applied, (b) EDX spectrum for the base plate and accompanying table of average EDX elemental mass percentages, with Boron excluded to minimise systematic error.*

The base plate was only very slightly magnetic, alluding to it being austenitic or martensitic. VLM performed on the base plate shows that it is likely an austenitic stainless steel due to the presence of polygonal grains with some annealing twins visible[23] in *Figure 3a.* Due to varying grain sizes within the microstructure, it can be surmised that the steel was only slightly cold-rolled (as cold rolling typically results in equiaxed grains of more uniform size[24]) and then annealed at a high temperature[25]. Though the microstructure in *Figure 3a* also resembles that of 316 and 304 austenitic stainless steels, it has smaller grains on average, that indicate it must be 201 stainless steels. An average grain diameter of 12.0 ± 4.5 µm was manually calculated when 100 grains were analysed using ImageJ in *Figure 3*; this aligns closely with literature values of 8.5 ± 4 µm[26]. The base plate sample has an average Vickers hardness of 227.3 ± 6.2 HV, which is consistent with literature values for ¼ hard cold-worked 201 stainless steels[27,28].

Point EDX performed on the base plate (see *Figure 3b*) showed similar composition to both 201 and 202 stainless steel[29,30], due to its uniquely high Manganese content; however the sample contained just over 1% Nickel (See *Figure 3b*) which is more consistent with 201 stainless steel – 202 stainless steels have 4 to 6% Nickel, while in 201 stainless steels minimal nickel is included, as it does not contribute to the mechanical properties other than stabilising the FCC austenitic phase[31]. It is of note that EDX data was skewed by very large readings for the presence of Boron (see *Appendix 2*), likely caused by the fact that EDX is inaccurate for low-atomic weight elements, especially those whose atomic weight is similar to Carbon (Boron is next to Carbon on the periodic table)[32]. This inaccuracy may have affected the EDX data and resulting conclusions, despite exclusion of Boron in calculations of composition. EDX data also shows slightly lower proportions of Manganese than expected for 201 austenitic stainless steels.

The use of 201 austenitic stainless steel for the base plate of the blender makes sense as it is one of the cheapest stainless steels on the market[33]. As the blender is on the lower end of the price range, the manufacturers likely chose the cheapest available steel with the desired properties. The steel is likely to be of very low grade, as its composition is not exactly like that of any other stainless steel, but rather only most closely aligned with 201 stainless steels, alluding to scrap steel being used, or a non-meticulous manufacture process. The microstructure and hardness also indicate only

slight cold rolling, meaning little attention was likely paid to the quality of the steel. 201 steels tend to be less corrosion resistant[33] and crack resistant[34] than other stainless steels, especially when heated. Given that the base plate is in close proximity to the motor, which tends to overheat and takes a long time to cool (as mentioned in the preliminary report), it is likely that crack formation in the base plate – either due to heat/stress or corrosion – is responsible for dents and leakages into the electricals below.

3.2 Polymers

Table 1. *Averaged density and Shore A & D durometer hardnesses for key components – hardness tested on both faces of 1cm x 1cm flat samples. Values rounded to 2 decimal places.*

Component	Density (g/m^3)	Durometer Hardness	
		Shore D	Shore A
Female Blender Gear	1.38	75.7	-
Male Blender Gear	1.29	30.6	83.8
Casing	1.62	71.7(I), 74.9 (O)*	-
Base plate	1.70	79.4	-
O-ring	1.15	-	67.5

*Two hardness were attained, inside (I) and outside (O) faces of the material.

3.2.1 Male Blender Gear

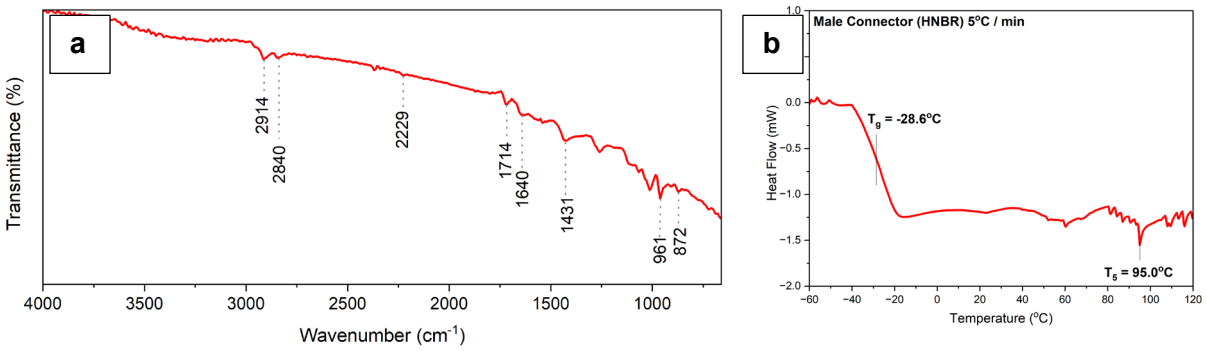

Figure 4. *(a) FTIR and (b) DSC graphs for the male blender, matching closely (99.3%) to Carbon-Black Hydrogenated Nitrile Butadiene Rubber (HNBR). The DSC graph was baseline corrected using Origin.*

The male gear's IR spectrum in *Figure 4a* had a near-perfect 99.3% match to Nitrile Butadiene Rubber (NBR) with medium ACN content (~30%), indicating its high purity. Relative wavenumbers that characterised this material included: C-H stretching peak at 2914 and 2480 cm^{-1}, a weak C≡N stretching peak at 2229cm^{-1}[35], C=O and C=C stretching peaks at 1714 cm^{-1} and 1640 cm^{-1} respectively, a peak at 1431 cm^{-1} was attributed to -CH_2- deformation vibration, and peaks at 961 and 872 cm^{-1} were related to C=C bending[35,36]. The weak transmittance drop at 1714cm^{-1} for C=O may indicate the presence of oxidation of NBR[36], as the main chemical structure doesn't contain such bonds inherently. As seen in DSC in *Figure 4b*, only one T_g value at -28.6°C was detected across testing a wide range of temperatures (including ones in *Appendix 3*), indicating this component is a random copolymer. This low temperature was expected, given the majority is polybutadiene – a polymer that is flexible due to its many σ bonds across C-H and C-C. In relation to the UTEN blender this is a concern; the component is at least above room temperature and in operation, the temperature will increase due to friction. Therefore, these temperatures will only accelerate the wear of HNBR (thermal wear) and shorten its lifespan.

The presence of additives was seen across both tests, most notably across the baseline of the IR spectrum. The gradual decrease in transmittance is due to the presence of carbon black[37]. This phenomenon occurs as light penetrates deeper at lower wavenumber area when using ATR[38]. It was seen that increasing carbon black content in HNBR improves the overall tear resistance, which is very desirable for its intended application, coming into frequent abrasion at operation. As seen the DSC graph in *Figures 4a* and *b (See Appendix 4)*, there were also microscopic endothermic and exothermic melting peaks at T_5, T_3, and T_4 (see latter two in *Appendix 5*) which indicated other additives such as steric acid, sulfur and peroxides which are all part of the vulcanization process[39], commonly done in manufacture for rubber compounds. The combination of such chemicals permits and reinforces cross-linking between HNBR amorphous chains, strengthening its mechanical properties - Young's modulus, compressive limit and more[40]. However, carbon black and its additives did not seem to make a significant impact on the hardness of the male blender gear. Referring to *Table 1*, its Shore D hardness was less than half that of the female blender gear (30.6 < 75.7) therefore regarded as a soft, more flexible and more prone to accelerated wear. There were few materials improvements to be made; rather that the geometry of this component was made poorly for its function in the blender and should be redesigned – its 'shark' tips should be revamped due to poor surface area for high abrasion rate. Had the group been able to access advanced characterisation techniques such as the Taber Abrasion Test[41], a more quantitative result could have aided the subgroup in optimising a redesign direct to the products function.

3.2.2 Base Plate (Polymer Surface) & Female Blender Gear

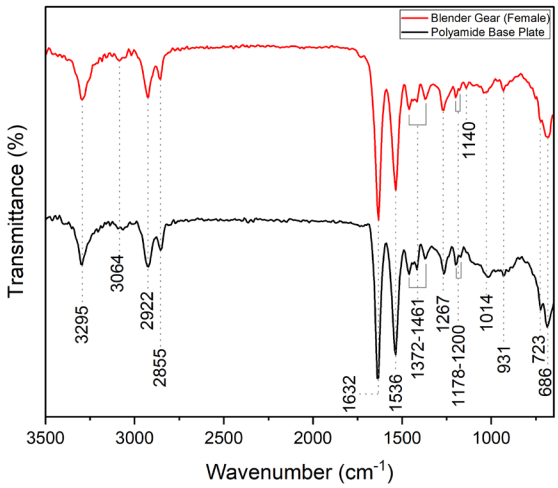

Both the female blender gear and the base plate were identified as polyamide with 96.9% and 89.0% matches respectively, evidenced by the characteristic peaks N-H stretching at 3295 cm^{-1}, aromatic C-H stretching at 3064 cm^{-1}, asymmetric and symmetric CH_2 stretching at 2922 and 2855 cm^{-1}, primary amide C=O stretching at 1632 cm^{-1}, secondary amide C-N stretching and N-H bending at 1536 cm^{-1}, and several tertiary amide peaks from 1372 to 1461 cm^{-1} and 1178 to 1200 cm^{-1}[42,43]. Additionally, asymmetric and symmetric C-O-C stretching peaks at 1267 and 1014 cm^{-1} were observed[43]. Peaks at 931 cm^{-1} and 686 cm^{-1} corresponded to amide IV and V vibration modes[44], providing further evidence of the polyamide components. The peak at 723 cm^{-1} was attributed to $-(CH_2)_n-$, where $n \geq 4$[45].

One peak at 1140 cm^{-1}, present only in the female blender gear, was of particular interest. While a definitive conclusion could not be reached, the most likely sources were determined to be the P=O stretching from triphenyl phosphate[46], a common flame retardant, or the Si-O-C stretching from silane coupling agents typically added when glass fibre or other infill materials are used[47]. Furthermore, densimetry on both components yielded densities higher than the typical PA density of around 1.1 g/cm^3[48] (Female gear - 1.38 g/cm^3, Base plate - 1.7 g/cm^3). Densimetry on both components yielded densities higher than the typical PA density of around 1.1 g/cm^3[48] (Female gear - 1.38 g/cm^3, base plate - 1.7 g/cm^3). This discrepancy could be explained by the presence of aromatic rings as aromatic PA can have a higher density, typically ranging from 1.3 to 1.5 g/cm^3[49], or potential infills used, which is congruent with the extra peak at 1140 cm^{-1}, as mentioned earlier.

3.2.3 Casing (Main Body)

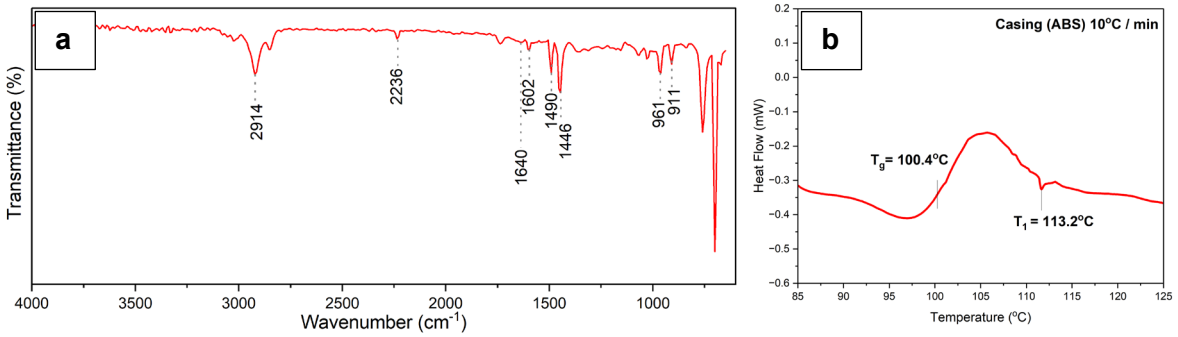

Figure 6. *(a) FTIR and (b) DSC graphs for the casing material, matching closely (90%) to Acrylonitrile Butadiene Styrene (ABS), plotted in Origin.*

The casing was identified as ABS (Acrylonitrile butadiene styrene) with 76.4% match. Peaks located at 2914 cm^{-1} showed the casing to be aromatic and possessing an aliphatic C-H stretch. C-N stretch mode of acrylonitrile is present at 2236 cm^{-1}; C=C stretching from poly(butadiene) appears at 1640 cm^{-1}, peaks at 1602 and 1490 cm^{-1} are due to the styrene ring, a peak at 1446 cm^{-1} is the scissoring mode of CH_2, and peaks at 961 and 911 cm^{-1} are C-H deformation in poly(butadiene)[50]. The nitrile group has a strong electronegativity which contributes to the high chemical stability and high strength of ABS[51]. Butadiene units are soft and flexible due to the long carbon chain; combination with styrene can increase the toughness of ABS[51]. The soft butadiene units absorb energy during impact.

Unlike carbon black HNBR, *Figure 6b* DSC showed a much higher glass transition temperature (100.4°C) mainly due to the benzene functional group of polystyrene, which increases rigidity and steric hindrance. Given G16's preliminary thermal tests, the recorded 50°C near the motor will unlikely cause reordering of structure which may lead to possible degradation. Moreover, it was noted the peak around this T_g was not related to crystallization because ABS is mostly amorphous, and rather from chain relaxation of this copolymer. Sulfur was also present in this sample with a 113.2°C endothermic peak, which the temperature differs to HNBR due to ABS bonding environment being very different. For this application towards the product, enhancing cross-links improves its compression strength, idealistic for the material given consumers will hold the whole product firmly to move the blender across different kitchen environments.

With reference to *Table 1*, hardness values for ABS were lower than expected suggesting further additives such as plasticisers were incorporated. Using EDX or DSC would help specify the additives. With the outer face having a higher hardness, this is desirable since the outer face is more vulnerable into contact – such as human interaction or kitchen cutlery. The enhanced hardness indicates that a surface finish was applied – likely using polyurethane as it is cheaper to work with than UV curing.

3.2.4 O-ring

The O-ring was attached to the base plate and in contact with the cup to prevent leakage. It was identified by FTIR as PDMS, verified by the peaks (see *Appendix 9)*, including CH_3 stretching in Si-CH_3, deformation of CH_3 in Si-CH_3, Si-O-Si stretching at, and CH_3 rocking[52]. The CH_3 is hydrophobic, and Si-O-Si bonds have relatively high bond energy, hence giving the O-ring good chemical and thermal resistance[53]. Both bonds have high rotation angles, contributing to high flexibility and elasticity of the material.

4 Product Recommendations

This section details recommendations to enhance the UTEN 4 in 1 blender's overall functionality, durability and user satisfaction by analysing performance data and assessing user feedback. A number of improvements can be made, both to the materials used and the design of parts, to address the consumer complaints and shortcomings of the blender.

4.1 Blades

The blades should be angled to ensure efficient crushing to specifically target ice stuck below the blades which is a common issue decreasing blade longevity (See *Appendix 6*)[54]. 316 stainless steel is potentially a better material for blades than 304 stainless steel due to its superior corrosion resistance, enhanced strength, and better heat resistance[55]. The addition of molybdenum in 316 provides increased protection against corrosion, particularly from hard water[56]. Many consumers of low-cost blenders live in UK areas with hard water supply or do not invest in water filters, which might be the cause of such numerous reports of blade damage; mineral-rich water can lead to pitting corrosion and make steel more brittle[57]. Additionally, 316 stainless steel's ability to perform well at higher temperatures makes it ideal for blades exposed to high-heat conditions, i.e., near the motor. However, 316 stainless steels can cost 20-30% more than 304 stainless steel due to the additional alloying elements[58,59].

4.2 Front Plate

The blender's front plate should be an insulating polymer like Polyphthalamide (PPA) to prevent unsafe heat dissipation, with high hardness to avoid denting. PPA would be less expensive than stainless steel, while also being easy to clean, as well as being corrosion-resistant, maintaining a sleek, sophisticated look while being cheap. A polymer exterior could serve as a cheaper 'trade-off', and the recovered funds could be used to invest in improving the blades[60].

4.3 Base Plate

Polycarbonate (PC) would be more suitable for the base plate; it provides structural stability from compressive deformation (caused by blending solid food) and reduces possible heat transfer by friction from the gears. PC is more lightweight with a density of 1.2 kg/m³, and is more economical and environmentally friendly with lower carbon emissions (see *Appendix 7)* than Polyamide (PA). PA's carbon fibre inclusions also make it harder to decompose and separate. The base plate should be redesigned (See *Appendix 10*) with a concave plate to divert water away, preventing leakage. As seen with other higher-end blenders, the base plate can be made of one material, making production costs much lower – no need for adhesives to attach the steel and polymer, and possibly an elimination of the use of PDMS for O-rings. Also, PC is excellent for injection moulding to create the complexity of this proposed design in large volumes. Using the same surface finish used in the outer ABS case will augment durability (via hardness) of the blender, increasing its lifespan.

4.4 Casing

ABS would be a good material for the casing. The copolymer blend has a T_g of 100.4°C, higher than the 50°C achieved by the motor. It also has a good chemical resistance to liquids (including dishwashing liquid), recyclability upon end of life or disposal and a degree of flexibility without sudden fracture. The ABS should have a thickness of at least 0.5 cm for the casing to prevent buckling and reduce thermal conduction. Alternatively, a thicker coating of polyurethane or epoxy applied through multiple dip coatings could provide protection and a smooth outer surface[61].

4.5 Male Blender Gear

UHMWPE (Ultra High Molecular Weight Polyethylene) could be used due its high hardness compared to NBR[62], meaning it is less likely to deform or wear under the abrasive conditions in the blender[63], It is also recyclable and carries low friction so energy transfer will be efficient.

4.6 Additional Recommendations

Improvements can be made to other aspects of the blender if the manufacturing budget were to be expanded. Primarily, a replacement of the motor with a more efficient[64] (albeit more expensive) one would prevent the blender from overheating while also ensuring a more thorough blend due to more rotations per minute (RPM). Interestingly, the most expensive and highly rated blenders promote the stainless-steel blades as dull, ensuring customer safety, therefore it can be said that expensive blenders use a higher RPM to ensure maximum blending efficiency.

The square jar design of popular blenders creates a blending vortex that enhances the performance of the blender. The square shape introduces corners and flat sides that disrupts the smooth flow of ingredients[65]. The disruption creates turbulence as the ingredients hit the sides and corners of the jar promoting more movement and circulation within the jar, specifically causing ingredients to be redirected to the centre, where the blades are. Increased turbulence and circulation also help to minimise the formation of air pockets (cavitation) around the blade. Additionally, all cups provided with the blender are made of polycarbonate, which typically contains bisphenol A (BPA) that is harmful to humans[66]. Improvements to the processing method, e.g., using dielectric barrier discharge to limit BPA migration[67] could be considered as an alternative to switching to other plastics.

5 Budget Spend Update

G16 kept characterization process under the £5000 budget proposed in the preliminary report. As seen in *Table 2*, the total spent was £4375, with £625 left over. While the group was able to achieve high-quality results and sufficient analyses across all tests, this expenditure was £1125 more than planned, due to limited VLM and Metal prep sessions (steel samples were not yet mounted at times, or the incorrect etchant was used from prior metal preparation sessions). Furthermore, some experimental errors were out of control, and prevented collection of useful information for analysis; e.g., in one DSC test, as a burnt heat detector in the machine saw an anomalous jump in heat flow around 180^{o}C at 10^{o}C per minute for the male blender gear sample (see *Appendix 11*). The former could easily be dealt with had the group distributed the tests more evenly throughout the characterization window to permit time for analysis, rather than compiling them in 1 week.

Table 2. *G16's cumulative expenditure of all experiments conducted and the associated total cost.*

Technique	Duration per session (h)	Cost per session (£)	Sessions	Cost (£)
SEM / EDX	1.0	750	1	750
FTIR	0.5	250	3	750
Hardness	0.5	250	2	500
DSC	0.5	250	5	1250
VLM	0.5	125	2	250
Metal Prep*	0.5	125	3	375
Densimetry	0.5	50	3	150
Etchants**	0.5	50	2	100
			Total Cost	4125

*involves cutting, mounting, grinding and polishing.
**pricing based per etchant used.

6 References

[1] M. A. Meyers, K. K. Chawla, *Mechanical Behavior of Materials*, Cambridge University Press, **2008**.

[2] Tianrui Zheng, Mervyn Ochoa-Dugoy, Nick Martin, Isabella Wu, Saiful Islam, Francesca Manyonyi, *MATE50003 ENGINEERING PRACTICE Preliminary Report*, London, **2024**.

[3] G. F. Vander Voort, Buehler Ltd., Lake Bluff, **2003**.

[4] J. Schindelin, I. Arganda-Carreras, E. Frise, V. Kaynig, M. Longair, T. Pietzsch, S. Preibisch, C. Rueden, S. Saalfeld, B. Schmid, J.-Y. Tinevez, D. J. White, V. Hartenstein, K. Eliceiri, P. Tomancak, A. Cardona, *Nat Methods* **2012**, *9*, 676.

[5] OriginLab Corporation, “Origin(Pro) 2024,” **2024**.

[6] Inc. ANSYS, “Ansys GRANTA EduPack Software,” **n.d.**

[7] S.-J. Lee, Y.-K. Lee, A. Soon, *Appl Surf Sci* **2012**, *258*, 9977.

[8] thyssenkrupp, “Stainless Steel 304 1.4301,” can be found under https://www.thyssenkrupp-materials.co.uk/stainless-steel-304-14301.html, **n.d.**

[9] V. Bedekar, R. Voothaluru, D. Yu, A. Wong, E. Galindo-Nava, S. B. Gorti, K. An, R. S. Hyde, *Int J Plast* **2020**, *131*, 102748.

[10] S. Sai Rakesh Singh, R. Venkata Praneeth, V. Sai Sankalp, S. Sravan Sashank, R. Karthikeyan, *Mater Today Proc* **2022**, *62*, 3675.

[11] K. Nomura, Y. Ujihira, *J Mater Sci* **1990**, *25*, 1745.

[12] J. Arrizubieta, A. Lamikiz, M. Cortina, E. Ukar, A. Alberdi, *Int J Mach Tools Manuf* **2018**, *135*, DOI 10.1016/j.ijmachtools.2018.08.004.

[13] C. Zheng, C. Liu, M. Ren, H. Jiang, L. Li, *Materials Science and Engineering: A* **2018**, *724*, 260.

[14] Z. Zhang, H. Zhang, X. Liu, T. Wang, Q. Huang, X. Liao, *J Manuf Process* **2023**, *108*, 764.

[15] T. R. Bieler, P. Eisenlohr, C. Zhang, H. J. Phukan, M. A. Crimp, *Curr Opin Solid State Mater Sci* **2014**, *18*, 212.

[16] A. Amininejad, R. Jamaati, S. J. Hosseinipour, *Materials Science and Engineering: A* **2019**, *767*, 138433.

[17] Matmatch, “Ferritic Stainless Steel: Properties, Grades, and Applications,” can be found under https://matmatch.com/learn/material/ferritic-stainless-steel, **n.d.**

[18] Hobart Filler Metals, “Stainless Steel Technical Guide - Class II - Ferritic Stainless Steels,” can be found under https://www.hobartbrothers.com/resources/technical-guides/stainless-steel-technical-guide/class-ii-ferritic-stainless-steels/, **n.d.**

[19] J. M. Gonzalez-Leal, E. Gallero, E. Blanco, M. R. del Solar, A. Núñez, J. Almagro, *Metals (Basel)* **2021**.

[20] N. Sommer, F. Stredak, M. Wiegand, S. Böhm, *Welding in the World* **2023**, *67*, 51.

[21] Shane, “Stainless Steel Hardness Table,” can be found under https://www.machinemfg.com/stainless-steel-hardness-table/?utm_content=cmp-true, **2023**.

[22] thyssenkrupp, “What is the difference between 304 and 430,” can be found under https://www.thyssenkrupp-materials.co.uk/the-difference-between-stainless-steel-304-and-430.html, **n.d.**

[23] Steel., *An Overview of Welded Low Nickel Chrome-Manganese Austenitic and Ferritic Stainless Steel*, **2016**.

[24] H. Zhu, A. K. Ghosh, K. Maruyama, *Materials Science and Engineering: A* **2006**, *419*, 115.

[25] A. Kisko, A. Hamada, L. P. Karjalainen, J. Talonen, **2011**.

[26] M. Khedr, I. R. Ibrahim, M. Jaskari, M. Ali, H. A. Abdel-Aleem, T. S. Mahmoud, A. Hamada, *Materials (Basel)* **2023**, *16*.

[27] AK Steel, *201 Stainless Steel*, **n.d.**

[28] Taylor Special Steels Ltd, “CONVERSION CHART OF VICKERS HARDNESS (HV) TO ROCKWELL C (HRC),” can be found under http://www.taylorspecialsteels.co.uk/pages/main/conchart.htm, **n.d.**

[29] Combined Metals Company, “201 Stainless Steel,” can be found under https://www.combmet.com/201-stainless-steel-alloy/#:~:text=Properties%20of%20Type%20201%20Steel,Nickel%20than%20type%20304%20steel, **n.d.**

[30] Y. Agrawalla, “Optimization of machining parameters in a turning operation of austenitic stainless steel to minimize surface roughness and tool wear,” can be found under https://api.semanticscholar.org/CorpusID:135413818, **2014**.

[31] M. Sehgal, “How does Nickel act as an austenitic stabilizer for Stainless steel?,” **2014**.

[32] CERN, “Energy Dispersive X-ray Spectroscopy (EDX),” can be found under https://en-mme-mm.web.cern.ch/content/energy-dispersive-x-ray-spectroscopy-edx#:~:text=It%20is%20important%20to%20highlight,Z%20between%204%20and%2011, **n.d.**

[33] Tuofa, “Comparing 201 and 304 Stainless Steel: Properties, Uses, and Cost Analysis,” **2024**.

[34] aalco, “Stainless Steel - Austenitic - 201~201L~202~204,” can be found under https://www.aalco.co.uk/datasheets/Stainless-Steel-201201L202204_97.ashx, **2018**.

[35] LibreTexts Chemistry, “Infrared Spectroscopy Absorption Table,” **n.d.**

[36] J. Liu, X. Li, L. Xu, P. Zhang, *Polym Test* **2016**, *54*, 59.

[37] Shimadzu, “Effects of carbon black, etc. (ATR method),” can be found under https://www.ssi.shimadzu.com/service-support/faq/ftir/5/index.html, **n.d.**

[38] Shimadzu, “Points to Note in Rubber Analysis : Black Rubber,” can be found under https://www.shimadzu.com/an/service-support/technical-support/ftir/tips_and_tricks/rubber.html, **n.d.**

[39] Anne Helmenstine, “Vulcanization of Rubber,” can be found under https://sciencenotes.org/vulcanization-of-rubber/, **2021**.

[40] Special Chem, “Selecting Carbon Black for Plastics,” can be found under https://polymer-additives.specialchem.com/selection-guide/selecting-carbon-black-for-plastics, **n.d.**

[41] S. Suzuki, E. Ando, *Thin Solid Films* **1999**, *340*, 194.

[42] F. Mallamace, C. Corsaro, D. Mallamace, S. Vasi, C. Vasi, G. Dugo, *Comput Struct Biotechnol J* **2014**, *13*, DOI 10.1016/j.csbj.2014.11.007.

[43] C.-W. Chang, G.-S. Liou, S.-H. Hsiao, *Journal of Materials Chemistry - J MATER CHEM* **2007**, *17*, DOI 10.1039/b613140a.

[44] L. Tao, K. Liu, T. Li, R. Xiao, *Polymer Bulletin* **2020**, *77*, 1135.

[45] J. Farias-Aguilar, M. Ramírez Moreno, L. Téllez-Jurado, H. Balmori-Ramírez, *Mater Lett* **2014**, *136*, 388.

[46] NIST, “Triphenyl phosphate,” can be found under https://webbook.nist.gov/cgi/cbook.cgi?ID=C115866&Type=IR-SPEC&Index=1#Top, **n.d.**

[47] Shin-Etsu Silicone, *Silane Coupling Agent - Combination of Organic and Inorganic Materials*, **n.d.**

[48] M. Palabiyik, S. Bahadur, *Wear* **2000**, *246*, 149.

[49] J. L. Santiago García, M. I. L. Bastarrachea, M. de Jesús Aguilar Vega, *Macromol Symp* **2013**, *325–326*, 120.

[50] R. A. N. D. A. C. A. N. D. G. G. A. N. D. M.-J. B. A. N. D. T. O. A. N. D. S. V. Desrousseaux Camille AND Cueff, *PLoS One* **2015**, *10*, 1.

[51] LibreTexts, “Chemistry of Nitriles,” can be found under https://chem.libretexts.org/Bookshelves/Organic_Chemistry/Organic_Chemistry_(Morsch_et_al.)/20%3A_Carboxylic_Acids_and_Nitriles/20.07%3A_Chemistry_of_Nitriles, **n.d.**

[52] L. M. Johnson, L. Gao, C. W. Shields IV, M. Smith, K. Efimenko, K. Cushing, J. Genzer, G. P. López, *J Nanobiotechnology* **2013**, *11*, 22.

[53] LibreTexts Chemistry, “Comparison Between Silicon and Carbon,” **n.d.**

[54] Dushan Sharendra De Seram, “A Deep Dive into the Blender Blade Assembly,” can be found under https://dushandt99.medium.com/a-deep-dive-into-the-blender-blade-assembly-646e3876fce5, **2023**.

[55] B. Kannan, T. Kumaran, U. Marimuthu, P. Padmanabhan, *INCAS BULLETIN* **2020**, *12*, 221.

[56] F. Ostovan, E. Shafiei, M. Toozandehjani, I. F. Mohamed, M. Soltani, *Journal of Materials Research and Technology* **2021**, *13*, DOI 10.1016/j.jmrt.2021.05.095.

[57] World Heat Cylinders, *Corrosive Effects of Chemicals on Hot Water Cylinders*, **n.d.**

[58] Silicon Steels, “316 stainless steel sheet price list,” can be found under https://www.siliconsteelalloys.com/stainless-steel-316-sheet-plate-supplier-stockist.html, **n.d.**

[59] Sanghvi Enterprise, “Stainless Steel Sheet Price List,” can be found under https://www.sanghvienterprise.com/stainless-steel-sheet-price-list.html, **n.d.**

[60] Syensqo, “An Advanced Portfolio of High-Performance Polymers for Food Contact,” can be found under https://www.syensqo.com/en/solutions-market/consumer-goods/household-goods/cooking-appliances/products#:~:text=Amodel%C2%AE%20PPA%20outperforms%20standard,exposed%20to%20water%20and%20steam., **n.d.**

[61] Nick Shusan, “Epoxy Vs Polyurethane Coatings: A Comprehensive Comparison,” can be found under https://epoxytimes.com/epoxy-vs-polyurethane/, **2022**.

[62] Hoffmann, “Acrylonitrile butadiene rubber (NBR),” can be found under https://www.hofftech.com/en/rubber-lexicon/nbr/#:~:text=NBR%20rubber%20is%2C%20however%2C%20not,resistant%20seals%2C%20membranes%2C%20hoses., **n.d.**

[63] T. D. L. M. Ramírez, I. Hilerio, M. Doñu Ruiz, N. López Perrusquia, E. D. García Bustos, M. Flores Martínez, *Modeling and Numerical Simulation of Material Science* **2020**, *10*, 1.

[64] Consumer Reports, “Blender Ratings,” can be found under https://www.consumerreports.org/appliances/blenders/, **n.d.**

[65] Emily Farris, “Why the Shape of Your Blender Pitcher Matters: A Not-Too-Nerdy Deep Dive,” can be found under https://www.epicurious.com/shopping/why-the-shape-of-your-blender-pitcher-matters, **2022**.

[66] V. McGovern, *Environ. Health Perspect.* **2009**, *117*, A406.

[67] M. Mohy Eldin, E. Soliman, A. Samir, A. Hassan, G. Naeem, *Open Journal of Synthesis Theory and Applications* **2014**, *3*, 27.

7 Appendices

7.1 Appendix 1 – Image of some of the cut, mounted, ground, polished and etched samples.

7.2 Appendix 2 - Unchanged elemental composition data from point EDX on Base.

Element	Mass %
Cr	7.3
Mn	4.6
Fe	33.6
Ni	0.7
Si	0.1
B	53.9

7.3 Appendix 3 – DSC Data for the male blender gear.

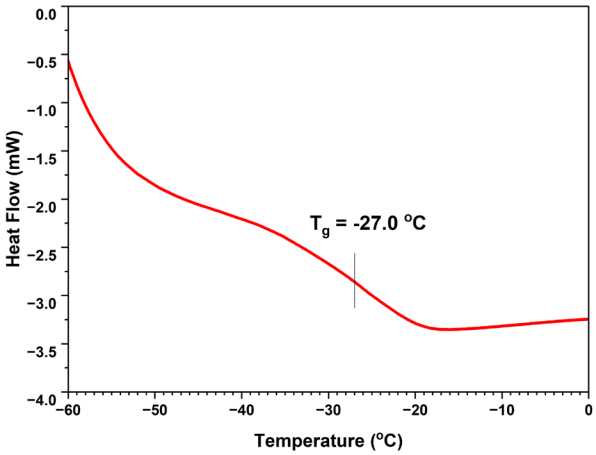

7.4 Appendix 4 – DSC Data for the male blender gear, showing T_5.

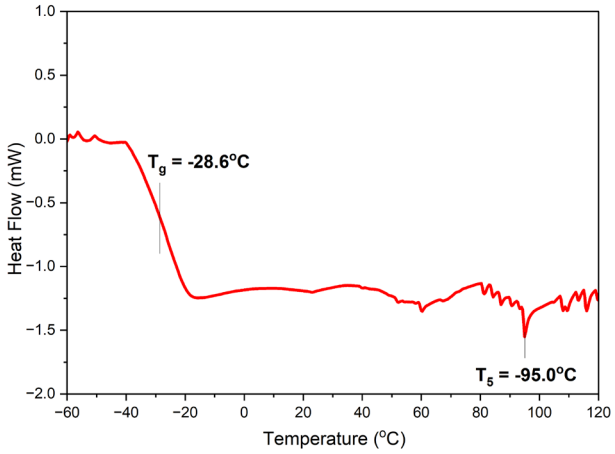

7.5 Appendix 5 – DSC Data for the male blender gear, showing T_3 and T_4.

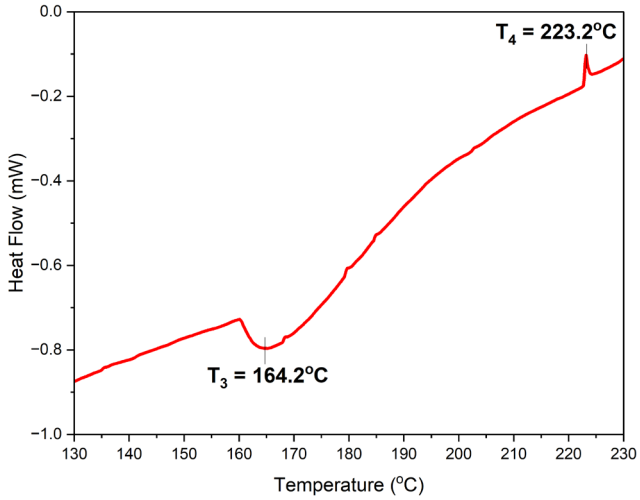

7.6 Appendix 6 – Ideal blade design for crushing ice.

7.7 Appendix 7 – Data on various properties of PC compared to PA

Material	Base Plate	
	Polycarbonate (PC)	**PA 66/6 (60% Glass Fibre)**
Composition	100% thermoplastic polymer	40% PA, 60% Glass Filler
Price per volume (x10^3 GBP/m^3)	2.21 - 2.87	3.36 - 4.65
Hardness*	V 18 - 20	V 36.4 - 40.2
Density (x10^3 kg/m^3)	1.19 - 1.21	1.64 - 1.72
Shear modulus (GPa)	0.829 - 0.872	4.92 - 6.11
Young modulus (Gpa)	2.32 - 2.44	13.2 - 16.4
Specific heat capacity (x10^3 J/kgC)	1.15 - 1.25	1.84
Glass Transition Temperature (C)	142 - 158	53 - 55
Melting Temperature (C)	226 - 322	255 - 265
Injection Moulding	Excellent	Limited Use
Molding energy (MJ/kg)	18.7 - 20.6	24.1 - 26.6
Recyclability	Yes	No
Other notes	Very good chemical resistance Amorphous structure	Optically opaque Semi-crystalline structure

Material	Male Blender Gear	
	HNBR (25-40% carbon black)	**UHMWPE**
Composition	50-70% HNBR 5-10% plastiziser 25-40% carbon powder	100% thermoplastic polymer
Price per volume (x10^3 GBP/m^3)	1.26 - 1.49	1.05 - 1.26
Hardness*	V 5 - 9, A 62-80	V 6 - 8
Density (x10^3 kg/m^3)	1.13 - 1.22	0.931 - 0.949
Shear modulus (GPa)	0.0015 - 0.0033	0.314 - 0.339
Young modulus (Gpa)	0.0045 - 0.01	0.894 - 0.963
Specific heat capacity (x10^3 J/kgC)	1.48 - 1.70	1.75 - 1.81
Glass Transition Temperature (C)	-60 to -10	-125 to -90
Melting Temperature (C)	-	180 - 280
Injection Moulding	Acceptable	Limited Use
Molding energy (MJ/kg)	16.3 - 18.0	21.1 - 23.3
Recyclability	No	Yes
Other notes	Partial or fully hydrogenated Toxic	Excellent durability Semi-crystalline structure

7.8 Appendix 8 – Table of hardness values HV for each steel component.

Test	Front Plate (HV)	Base Plate (HV)	Blade (HV)
1	147	245	355
2	137	225	330
3	145	217	320
4	151	222	346
5	153	214	334
6	158	216	329
7	146	239	293
8	147	222	306
9	147	231	337
10	156	242	341

7.9 Appendix 9 – FTIR spectrum of the O-ring with peaks identified and labelled.

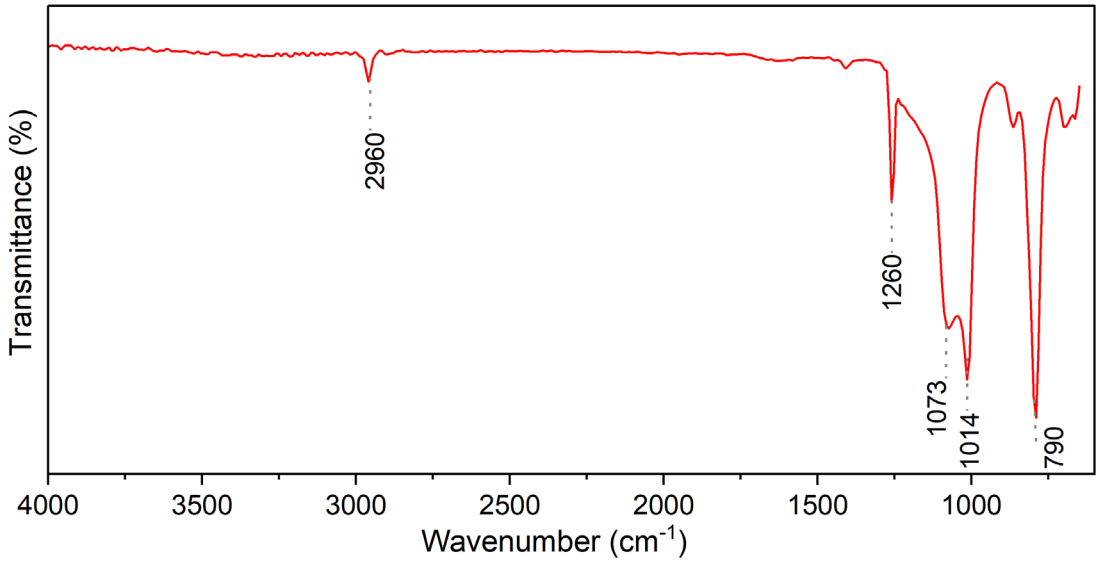

Wavenumber (cm^{-1})	Bond
2960	Asymmetric CH_3 stretching in Si-CH_3
1260	CH3 deformation in Si-CH_3
1703,1014	Si-O-Si stretching
790	CH_3 rocking in Si-CH_3

7.10 Appendix 10 – Redesigned base plate.

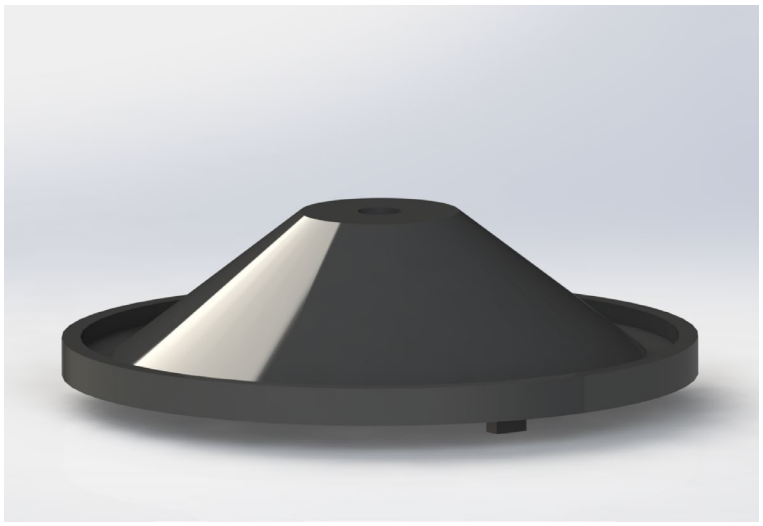

7.11 Appendix 11 – Redesigned male gear.

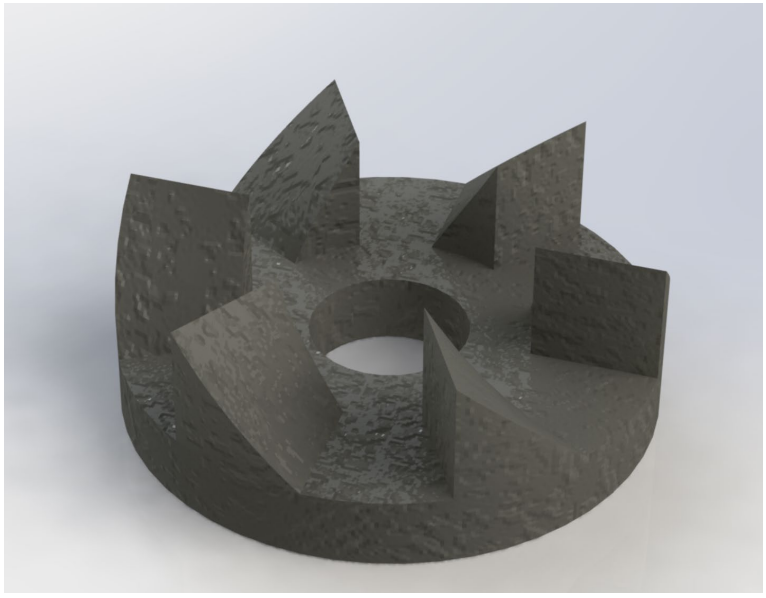

7.12 Appendix 12 – Updated Gantt chart of project progression.

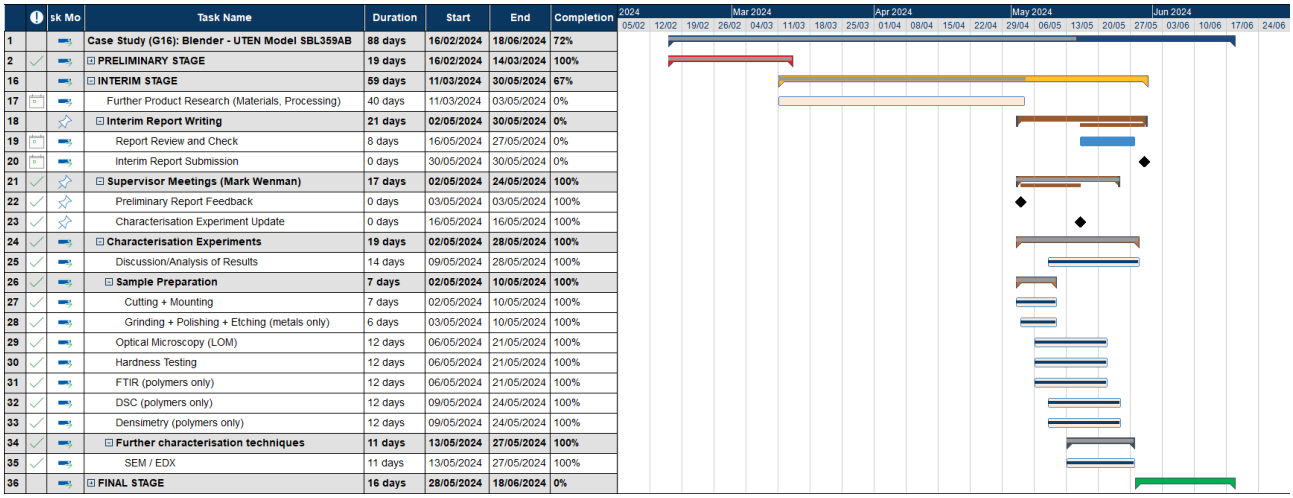

		sk Mo	Task Name	Duration	Start	End	Completion
1			**Case Study (G16): Blender - UTEN Model SBL359AB**	**88 days**	**16/02/2024**	**18/06/2024**	**72%**
2	✓		**PRELIMINARY STAGE**	**19 days**	**16/02/2024**	**14/03/2024**	**100%**
16			**INTERIM STAGE**	**59 days**	**11/03/2024**	**30/05/2024**	**67%**
17			Further Product Research (Materials, Processing)	40 days	11/03/2024	03/05/2024	0%
18			**Interim Report Writing**	**21 days**	**02/05/2024**	**30/05/2024**	**0%**
19			Report Review and Check	8 days	16/05/2024	27/05/2024	0%
20			Interim Report Submission	0 days	30/05/2024	30/05/2024	0%
21	✓		**Supervisor Meetings (Mark Wenman)**	**17 days**	**02/05/2024**	**24/05/2024**	**100%**
22	✓		Preliminary Report Feedback	0 days	03/05/2024	03/05/2024	100%
23	✓		Characterisation Experiment Update	0 days	16/05/2024	16/05/2024	100%
24	✓		**Characterisation Experiments**	**19 days**	**02/05/2024**	**28/05/2024**	**100%**
25	✓		Discussion/Analysis of Results	14 days	09/05/2024	28/05/2024	100%
26	✓		**Sample Preparation**	**7 days**	**02/05/2024**	**10/05/2024**	**100%**
27	✓		Cutting + Mounting	7 days	02/05/2024	10/05/2024	100%
28	✓		Grinding + Polishing + Etching (metals only)	6 days	03/05/2024	10/05/2024	100%
29	✓		Optical Microscopy (LOM)	12 days	06/05/2024	21/05/2024	100%
30	✓		Hardness Testing	12 days	06/05/2024	21/05/2024	100%
31	✓		FTIR (polymers only)	12 days	06/05/2024	21/05/2024	100%
32	✓		DSC (polymers only)	12 days	09/05/2024	24/05/2024	100%
33	✓		Densimetry (polymers only)	12 days	09/05/2024	24/05/2024	100%
34	✓		**Further characterisation techniques**	**11 days**	**13/05/2024**	**27/05/2024**	**100%**
35	✓		SEM / EDX	11 days	13/05/2024	27/05/2024	100%
36			**FINAL STAGE**	**16 days**	**28/05/2024**	**18/06/2024**	**0%**

7.13 Appendix 13 – Table of individual contributions.

Name	Contribution
Saiful Islam	Steels (blade + base + front) sample preparation and characterisation, recommendations
Francesca Manyonyi	Steels (blade + base + front) sample preparation and characterisation, (steels) base plate and front plate results analysis and conclusions, executive summary, introduction and recommendations, proofreading and editing report, image formatting, appendices
Nick Martin	Steels (blade + base + front) sample preparation and characterisation, plotting data, results/data analysis, conclusions, and recommendations, CAD redesign, graphs, tables, microstructure images(Image J analysis), proofreading and editing report.
Mervyn Ochoa-Dugoy	Polymer sample preparation, Polymers characterisation, DSC graphs and data analysis, introduction, recommendations, budget spend update, proofreading and editing report
Isabella Wu	Polymer sample preparation, Polymers characterisation, data analysis, FTIR graph plotting, proofreading and editing report
Tianrui Zheng	Polymer sample preparation, Polymers characterisation, data analysis, FTIR graph plotting referencing, proofreading and editing report